



Microbial electrochemical technologies: Electronic circuitry and characterization tools

Title	Microbial electrochemical technologies: Electronic circuitry and characterization tools
Author(s)	Sánchez, Carlos; Dessì, Paolo; Duffy, Maeve; Lens, Piet N. L.
Publication Date	2019-11-16
Publisher	Elsevier
Repository DOI	10.1016/j.bios.2019.111884

Microbial electrochemical technologies: electronic circuitry and characterization tools

Carlos Sanchez ^{a*}, Paolo Dessì ^a, Maeve Duffy ^b, Piet N. L. Lens ^a

* Corresponding author: Carlos Sanchez, Email: c.sanchez2@nuigalway.ie Telephone: +34685626284

^a Microbiology department. School of Natural Sciences, National University of Ireland, Galway, University Road, Galway, Ireland.

^b Electrical and Electronic Engineering. School of Engineering, National University of Ireland, Galway, University Road, Galway, Ireland.

Abstract

Microbial electrochemistry merges microbiology, electrochemistry and electronics to provide a set of technologies for environmental engineering applications. Understanding the electronic concepts is crucial for effectively adopting these systems, but the importance of electronic circuitry is often overlooked by microbial electrochemistry researchers. This review provides the background on the electronics and electrochemical concepts involved in the study of microorganisms interacting with electricity, and their applications in microbial electrochemical technology (MET). The potentiostat circuitry is described along with its working principles. Electrochemical analyses are presented together with the rational and parameters employed to study MET devices and electroactive microorganisms. Finally, future directions are delineated towards the adoption of MET, and the related electronics, in environmental engineering applications.

Keywords: bioelectrochemical system, cyclic voltammetry, electrochemical impedance spectroscopy, electrode polarization, microbial fuel cell, potentiostat.

CONTENTS:

1. Introduction
2. Electrical and electrochemical background for MET
 - 2.1. Electron flow conventions
 - 2.2. Electrical ground
3. History of electrochemical measurement devices related to MET
4. Electrode potential control
 - 4.1. Effect of potential on microbial metabolism
 - 4.2. Potentiostat
 - 4.2.1. Working principle
 - 4.2.2. Potentiostat circuitry
 - 4.2.3. Limitations of the potentiostatic circuitry
5. Polarization analysis for MET
 - 5.1. Direct current techniques
 - 5.1.1. Chronoamperometry and chronopotentiometry
 - 5.1.2. Polarization sweep
 - 5.1.3. Linear sweep and cyclic voltammetry catalyst
 - 5.2. Alternating current techniques
 - 5.2.1. The concept of impedance
 - 5.2.2. Electrochemical impedance spectroscopy
6. Future perspectives for electronics in MET
7. Conclusions

1. Introduction

The electrical activity of microbes was discovered more than a century ago when microbes were shown to interact electrically with a platinum electrode (Potter, 1911). The electrochemical reactions derived from these microbial-electrode interactions resulted in the development of a broad number of biotechnological applications within the field of microbial electrochemical technology (MET) (Schröder et al., 2015). MET include electricity production from wastewater in microbial fuel cells (MFC), hydrogen or methane production in microbial electrolysis cells (MEC), elongation of CO₂ to volatile fatty acids (VFAs) in microbial electrosynthesis cells (MES) and low-cost desalination in microbial desalination cells (MDC) [Figure 1] (Borjas et al., 2017; Fangzhou et al., 2011; Rabaey and Rozendal, 2010). Nowadays, METs are applied in bioremediation (Lohner and Tiehm, 2009), extraction of scarce resources (Nancharaiyah et al., 2016; Varia et al., 2013) and sensing the environment for biological oxygen demand (BOD) or for the presence of contaminants (Su et al., 2011).

METs use various electronic components to control and measure the microbial metabolism and electrochemical reactions. During the twentieth century, electronic devices have been developed for a more reliable control of MET experiments, and several electrochemical techniques, such as polarization curve, cyclic voltammetry, and impedance spectroscopy, were introduced to the field (Dominguez-Benetton et al., 2012; Logan et al., 2006). Since most of these techniques are adapted from electrochemical methods, a background knowledge of electronics is required for an appropriate design and realization of the experiments. However, MET researchers often lack an adequate training on electronics, and electrical engineers are not aware of the specific requirements of METs. This review aims to provide the required electronic and electrochemical concepts for MET experiments, and the related electrochemical analyses, bridging the gap between electronics, electrochemistry and microbiology.

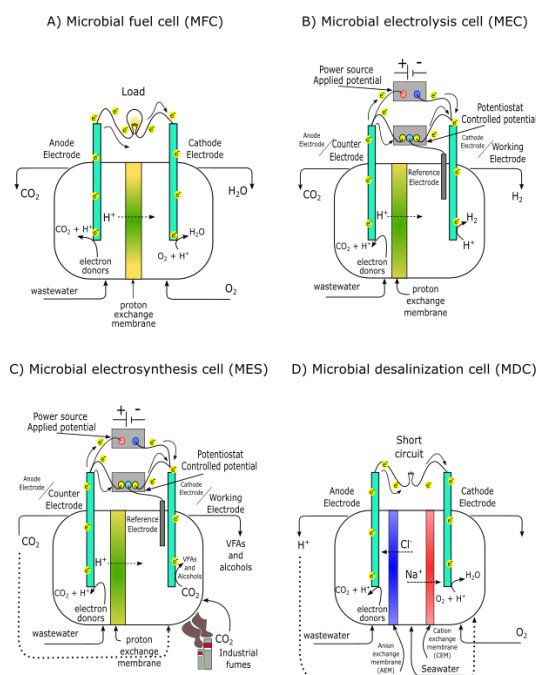


Figure 1: Overview of microbial electrochemical technologies (MET) applied to water and gas treatment. Microbial fuel cell (MFC) for electricity production from wastewater [A]; microbial electrolysis cell (MEC) [B], and microbial electrosynthesis cell (MES) [C] for cathodic production of hydrogen and VFA/alcohols, respectively, and microbial desalination cell (MDC) comprising both anion and cation exchange membranes to allow migration of salts [D]. MEC and MES require an energy input, e.g. using a power source or a potentiostat circuit, to drive the electrochemical transformations.

2. Electrical and electrochemical background for MET

2.1. Electron flow conventions

Around 1750, Benjamin Franklin described the flow of electricity as positive charges flowing towards negative particles (Franklin, 1751). Although a century after Franklin's experiment it was established that electricity is produced by a flow of negative charges (electrons), Franklin's convention is still used in the analysis of electrical systems, circuits and electronic components. In MET, however, the natural electron flow, from the anode towards the cathode, is used as a convention to facilitate the analysis of electrochemical transformations [Figure 2].

In electrochemistry, both conventions are used depending on the focus of the study. The convention based on the electron flow is used to analyse the chemical transformations and biological metabolism, whereas Franklin's convention is generally adopted to work on electronic circuitry. Familiarization with the electronic convention is necessary when modelling MET into circuit schematics, when using polarized components such as diodes, to avoid current reversal, or when designing energy harvesting circuits to convert the electric energy produced by MFCs into a usable form (Khaled et al., 2016; Zhu et al., 2011).

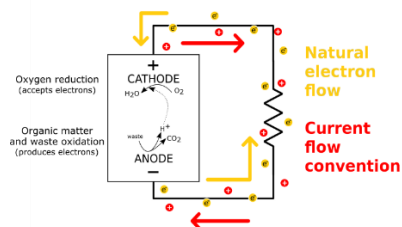


Figure 2: Difference between the natural electron flow and Franklin's current flow convention on a typical MFC set-up combining oxidation of organics at the anode to oxygen reduction at the cathode.

2.2. Electrical ground

Ground is the reference potential of an electrical circuit, corresponding to the potential of an electrical connection to earth, which acts as an infinite source or sink for electrons. Grounding is commonly a safety requirement in electrical installations, based on the fact that current tends to return to its source (Whitlock, 2008). Therefore, grounding of equipment provides a low resistance return path to the current flow avoiding unpredictable electrical deflections. In electrochemical methods, the utilization of external power supplies and high currents requires grounding for safety reasons. However, grounding and interconnection of instruments can result in the generation of interferences called ground loops. Ground loops are caused by low resistance loop connections of the ground rail, which act as antennas for environmental electromagnetic fields (Whitlock, 2008).

To avoid ground loops, all the earth wires of the instruments should connect to a common collector. In certain conditions, loops can be avoided disconnecting the ground connection of a device and reconnecting it through the ground connection of another device, avoiding multiple ground connections. This is a practical solution for connecting potentiostats to external devices such as motors (Shen et al., 2016). In such cases in which multiple ground connections are detrimental, a ground link is included on the device's design to facilitate the disconnection of the internal ground from the earth protection (Doelling, 2000). Furthermore, galvanic isolation (e.g. by transformers, opto-isolators and/or relays) can be used to interconnect equipment avoiding ground loops (Ledoux, 2011).

Any piece of conductor isolated from ground, including electrodes and cables, can act as an antenna, causing electromagnetic interference that can affect the electrochemical analysis (Morrison, 2016). A typical source of interference is the alternating current (AC) of the power installations, which can be identified due to its sinusoidal shape and typical frequency of 50 or 60 Hz. This interference can be rejected by synchronizing

the sampling rate of the measurement to the AC frequency, in what can be referred to as a digital filter (Dryden and Wheeler, 2015). Switch-mode power supplies and digital communication devices can generate interferences at high frequencies (30 – 70 kHz). Component drift due to temperature can also result in noisy measurements at low frequency (< 1 Hz). Modern devices counteract this issue by means of embedded temperature regulation circuits, requiring small stabilization times, in the order of minutes, before measurement (Doelling, 2000).

A Faraday cage, consisting of a volume enclosed by conductive material, blocks the electromagnetic noise avoiding contamination of the measurement signals (shielding). However, in MET experiments, the importance of shielding is often ignored and little attention is given to electromagnetic noise, except for low current experiments in which minimizing noise is required (Jiang et al., 2013). Faraday cages need to be grounded to remove the noise from mains (Morrison, 2016). However, when performing experiments in a Faraday cage, the signals need to be transported to the measurement equipment through cables susceptible to electromagnetic noise. Shielded cables are commonly used to avoid corrupting the low voltage signals and in certain occasions, the shield is fed with a buffered potential of the signal to reduce the noise in a method known as driven guard (Dryden and Wheeler, 2015).

In modern electrochemical devices, differential amplifiers are used to amplify differences between the input voltage level of the signals resulting in an efficient reduction of common interferences, such as ground loops, through a technique called common-mode rejection (Morrison, 2016). Furthermore, some differential amplifiers (instrumental amplifiers) include an initial voltage follower or voltage buffer step for each of the inputs, minimizing the loading of input signals, thus enabling detection of low current signals, such as those generated by (bio)sensors (Ma et al., 2016). Modern devices are also designed to rapidly transform signals to the less sensitive digital counterparts by integrated analog-to-digital converters (ADC) for posterior data-logging and analysis (Morrison, 2016).

3. History of electrochemical measurement devices related to MET

Microbial electroactivity was discovered in 1911 when Potter noticed electricity generation from the degradation of organic compounds by *Saccharomyces cerevisiae* and other microorganisms, which produced an electromotive force (EMF) similarly to a galvanic cell (Potter, 1911). Rudimentary versions of both analog and digital signal processing were used for this

experiment. Current was measured by an electromagnetic ammeter, quantifying the deflecting force caused by the electrical current [analog], whereas a Morse condenser-mediated signal [digital] was used to count the charge transferred (Potter, 1911).

During the 20th century, the discovery and progressive development of semiconductors and other solid state electronics, such as the transistor and the integrated circuit (IC) version of the operational amplifier (op-amp), opened new horizons for electrical measurements, configurations and applications (Enke, 2015). The op-amp enabled development of circuits to perform rapid mathematical operations, including summing or integration of signals. In 1954, Andrew Kay invented the digital voltmeter, improving the accuracy and reducing the cost of electric measurements. Digital voltmeters are based on a special type of ADC which integrates the difference between the tested voltage and a reference with the help of a clock signal (Markoff, 2014). Later, the introduction of solid-state circuitry decreased the manufacturing costs, resulting in a progressive substitution of analog measurement devices by their digital counterparts.

Measurement devices should allow retrieving signal information avoiding interference with the system analysed. During the first studies on electrochemistry, it was shown that applying a constant potential to an electrode does not imply having control over the potential at each electrode in the electrochemical cell. In 1925, Heyrovský introduced polarography, controlling the potential at one electrode with a small surface (polarizable) against a large surface counterbalance electrode (non-polarizable) (Heyrovský, 1925). In 1937, the invention of a valve circuit current control allowed to maintain a constant small current regardless of the EMF and resistance changes in the electrochemical cell, opening new possibilities for electrochemical experiments (Bruce and Hickling, 1937).

In 1952, Hans Wenking introduced a three electrode system characterized by electrode potential control by means of a feedback-controlled power source and a reference electrode: the potentiostat (Doelling, 1998). Potentiostats allow to set a voltage difference between a reference electrode and the electrode under study (working electrode) regardless of changes in electrolyte conductivity, electrode surface and resistance. Development of the potentiostatic hardware enabled control of variable electrode potentials in electrochemical cells, and the introduction of solid-state electronics increased speed, accuracy, range and signal-to-noise ratio of electrical signal measurements. Today, potentiostats are devices which combine analog and digital circuits by means of

ADC and digital-to-analog converters (DAC) in conjunction with modern computers, allowing complex and detailed electrochemical analyses (Doelling, 2000).

4. Electrode potential control

4.1. Effect of potential on microbial metabolism

In MET, electroactive microorganisms catalyse electrochemical transformations (Rabaey et al., 2008). The electrode potential defines the (bio)electrochemical reactions occurring under specific environmental conditions. An electrode acts as final electron acceptor when its potential is higher than the open circuit potential (OCP), e.g. the MFC anode, whereas it acts as electron donor when its potential is lower than the OCP, e.g. the MFC cathode. The electrode potential affect the microbial communities and their electron transfer mechanisms. Thus, potential control has been proposed to facilitate MFC start-up, promote degradation of specific compounds, or promote synthesis of organic compounds at the cathode (Chatterjee et al., 2019; Dennis et al., 2016; Nevin et al., 2010; Wang et al., 2009). Certain microorganisms can even adapt to the electrode potential by using different intracellular or extracellular proteins for electron transfer (Torres et al., 2009; Zhu et al., 2013), and some have shown reversibility, acting either as anodic or cathodic catalyst depending on the electrode potential applied (Pous et al., 2016).

4.2. Potentiostat

4.2.1. Working principle

The modern potentiostat/galvanostat is essentially an amplifier circuit designed to control two and three-electrode electrochemical cells. It can be used, for example, to set the potential of an electrode while measuring the current produced [potentiostatic mode], or set the current flow while monitoring the potential [galvanostatic mode]. Two-electrode systems, consisting of an anode and a cathode, can be used to retrieve information on the whole electrochemical cell behaviour (e. g. battery, fuel cell, resistor or diode). Beyond this, potentiostat-controlled three-electrode systems allow independent analysis of the anode or cathode electrode (i.e. working electrode, WE), independently of the electrochemical reactions occurring on the opposite electrode (i.e. counter electrode, CE).

Besides WE and CE, the three-electrode system includes a reference electrode (RE) consisting of a reversible, known electrochemical reaction against which the WE potential is compared. The standard RE, called the standard hydrogen electrode (SHE), is the reversible redox reaction of hydrogen ($H^+ + e^- \leftrightarrow 1/2$

H₂) at a platinum electrode at 25 °C, which has conventionally a potential of 0 V. The saturated mercury/mercurous chloride calomel reference electrode (SCE) and the silver/silver chloride reference electrode (Ag/AgCl) are generally more popular for MET experiments than SHE as they are easy to handle (no requirement for a gas, such as hydrogen), cheaper and easy to construct, less dependent on temperature, and relatively stable (Dong et al., 2012; Liang et al., 2011; Qiao et al., 2007; Wang et al., 2017). The SCE is based on the equilibrium between mercury ($\text{Hg}_{2}^{2+} + 2 e^{-} \leftrightarrow 2 \text{Hg}_{(l)}$) and mercurous chloride ($\text{Hg}_2\text{Cl}_{2(s)} + 2 e^{-} \leftrightarrow 2 \text{Hg}_{(l)} + 2 \text{Cl}^{-}$), which sets a potential around 250 mV vs. SHE in concentrated chloride media. The Ag/AgCl reference is the most popular reference in MET, due to the absence of mercury, and relies on the equilibrium between metallic silver ($\text{Ag}^{+} + e^{-} \leftrightarrow \text{Ag}_{(s)}$) and its partially soluble silver chloride salt ($\text{AgCl}_{(s)} + e^{-} \leftrightarrow \text{Ag}_{(s)} + \text{Cl}^{-}$) in concentrated chloride media. The reduction potential for this electrode is around 200 mV vs. SHE [in 3 M sodium chloride], although dependent on chloride salt concentration and temperature. The Ag/AgCl electrode is photo-sensitive and thus, it should not be exposed to light to avoid instability.

A salt bridge is often used to connect the electrolyte of the cell under study to the RE electrolyte, avoiding migration of salts inside or outside the RE which could affect the chemical balance and thus, the RE potential. In a three-electrode set-up, the resistance between the RE and the WE, known as the uncompensated resistance, causes an ohmic potential drop that can become significant at high currents. The potentiostat cannot compensate the resistance between RE and WE as this resistance is not involved on the feedback loop of the amplifier circuitry [section 4.2.2]. Thus, minimizing the distance between the WE and RE is recommended. A glass capillary (Luggin capillary) is used in certain electrochemical experiments to minimize the uncompensated resistance. However, it should be noted that both the Luggin capillary and the salt bridge can clog during long-term MET experiments, causing voltage drifts, and thus require maintenance (F. Zhang et al., 2011).

In a three-electrode system, when applying a voltage to the WE, the CE acts as source (for cathode WE) or sink (for anode WE) of electrons. Potential control can also be applied using a RE and a precise power supply in two-electrode systems, as was done in the first polarography experiments (Heyrovský, 1925). However, such an approach can be used only for short-term and low current experiments, since the RE would act both as reference and source or sink of electrons, affecting its stability (Bond, 2007). MET experiments are typically long (days and up to months) and thus require a separate RE. A CE with larger surface area

than the WE is recommended to avoid CE limitations when carrying out electrochemical experiments (Bard and Faulkner, 2001).

4.2.2. Potentiostat circuitry

Potentiostats set the electrode potential or the current flow by using a combination of operational amplifiers (op-amps) and other electronic components. The op-amp, also called differential amplifier, is a five-terminal electronic component which acts as a voltage-controlled voltage source. The op-amp consist of two terminals (V+, V-) for powering the device (often not shown in circuit schematics), two additional terminals (+, -) for sensing the input signals and a fifth terminal (e_o) to provide the amplified output signal [Figure 3]. Op-amps set the output voltage as a function of the difference between the positive (non-inverting) and negative (inverting) inputs. When the potential at the non-inverting input is higher than the one at the inverting input, the output signal will be positive with respect to the ground, whereas the signal will be negative when the inverting potential is higher.

To effectively use the op-amp, the output signal must be fed to the negative input (negative feedback), resulting in identical potential values between both inputs which remain effectively isolated between each other due to a non-direct electrical connection. This characteristic allows to configure potential control in electronic circuits. For example, if the positive terminal of the op-amp is connected to the ground, the negative terminal has the same ground potential but it is effectively isolated from it in what is known as virtual ground (Roberge and Lundberg, 2007). If a known voltage is applied between the negative terminal and point A, the op-amp will adjust its output to maintain a constant potential at point A regardless of changes in resistors R₁ and R₂ [Figure 3].

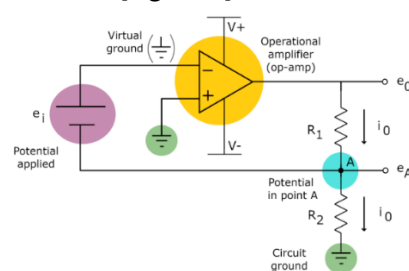


Figure 3: Circuit of the operational amplifier (op-amp) with the grounded positive terminal and the negative terminal at virtual ground. A voltage source at the negative input allows controlling the potential at point A regardless of changes in R₁ and R₂. The amplifier controls its output voltage, and thus the current, through the resistors so that the potential at point A equals the inverse of the potential applied (-e_i).

Potentiostats use a similar approach to the op-amp negative feedback [Figure 3] to control the potential, but with additional components and electrochemical counterparts [Figure 4]. The main component of a

potentiostat is the potential control amplifier [Figure 4: PC], an inverting amplifier acting similarly to the previously described op-amp configuration [Figure 3], comparing the RE and WE potentials. The multiple inputs at the summing amplifier [Figure 4: sum] of the potentiostat enable control of the WE potential in relation to the signal coming from the RE and allow the addition of other input signals. For example, wave generators can be added to the summing amplifier to perform sophisticated experiments, such as electrochemical impedance spectroscopy (EIS) [Section 5.2]. Applying AC waves requires a phase correction capacitor, as the amplification gain of the op-amp decreases with increasing frequencies of the input signal, while the phase shift increases (non-ideal slew rate), causing self-oscillating responses at specific frequencies which can harm the circuit and hamper the potential control. The phase correction capacitor [Figure 4: C_{phase}] prevents this malfunction by keeping the phase stable within the designated frequency range (Doelling, 2000). The relation between accuracy and frequencies depend on the op-amps and phase correction of the capacitor design, which may limit the possibilities for certain experiments as EIS (more on EIS in section 5.2). The limitations of each potentiostatic device are described by manufacturers in accuracy contour plots which define the range of measurable impedances, both for capacitive and inductive elements, including the expected percentage of error made on the measurement for the different excitation frequencies applied (Bio-Logic, 2015).

The RE potential is sensitive to loading, thus, most potentiostats use a voltage follower or voltage buffer consisting of an op-amp in non-inverting configuration, VF [Figure 4], which isolates the RE electrochemical reaction from the rest of the circuitry. An input resistor is often required to avoid static high voltage shocks that can damage the PC (Doelling, 2000). Despite these precautions, the Ag/AgCl RE can become unstable if used for a long time in a low conductivity electrolyte or under reductive conditions, which can lead to high concentrations and deposition of silver complex ions, which will clog the salt bridge (Inzelt et al., 2013). This can be particularly problematic in long-term reductive potentiostatic experiments, e.g. in MEC and MES, since an unstable RE causes undesired drifts at the WE.

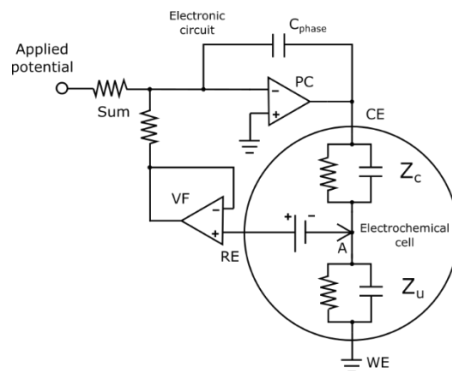


Figure 4: Circuit of the potential-controlled op-amp configuration of a potentiostat. The potential control (PC) amplifier maintains a constant potential at the point A. The RE acts as a voltage source between the controlled point A and the PC. This voltage is buffered by the voltage buffer (VF) amplifier to avoid loading that can affect the potential of the electrochemical voltage source. The impedance at the CE is compensated by the op-amp circuitry (Z_c) whereas the electrochemical cell under study generates an uncompensated impedance between the controlled point A and the ground (Z_u).

In potentiostats, current can be measured in different ways, depending on the type of grounding and power source [Figure 5]. The WE can be directly connected to the circuit's ground while measuring current by an instrumental amplifier, reducing noise pickup from additional components (resistor, op-amp) on the signal path of the potential control circuit. However, such configuration can limit the measurable current range, since high voltages at the current measuring resistor could exceed the limit of the instrumentation amplifier [Figure 5A]. An op-amp in current follower configuration can also be used to set the WE in virtual ground and thus, isolate it from the power ground (Figure 5B). Indeed, since the current tends to return to its source, this configuration allows to measure the current required to keep the set potential by monitoring the current flowing between the virtual and the power ground. Such current flow can be measured through a current shunt with respect to the power ground, avoiding the need for an instrumentation amplifier [Figure 5B]. Most common potentiostat configurations consist of a WE set at virtual ground and current measurement by means of a feedback current shunt resistor in a method known as "active shunt" [Figure 5C] (Bard and Faulkner, 2001; Doelling, 2000). Other types of grounding can be required for specific applications, with either CE or RE at virtual ground [Figure 5D] (Busoni et al., 2002; Meloni, 2016). High current configurations may require additional booster modules to increase the voltage capability on the PC amplifier, and current measurement amplifier circuits (Bard and Faulkner, 2001).

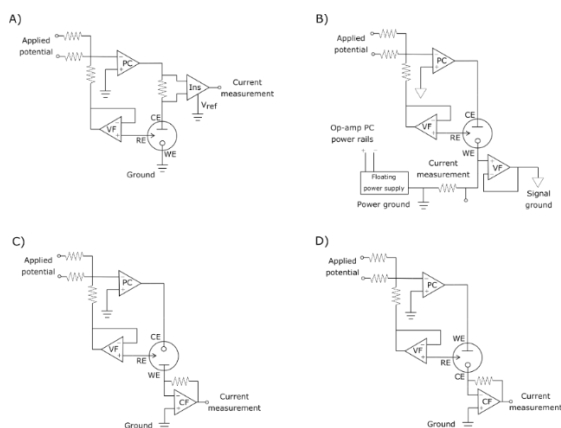


Figure 5: Different potentiostat configurations showing the three electrodes of electrochemical cells (CE, RE and WE) connected by operational amplifiers with different characteristics (PC, VF and CF). The potential control amplifier (PC) acts as a summing amplifier pooling the potential from RE and the applied potential signals. The voltage follower (VF) supplies the current required to avoid drawing current from the RE. An instrumentation amplifier (Ins) can be used to measure current [A]. The resistor between the signal ground (WE) and the power ground (floating power supply) carries the current required to maintain potentiostatic control [B]. The “active shunt” method relies on a current follower (CF) and a current shunt resistor to measure current without impacting the potential control [C]. Some experiments may require a grounded RE or CE [D].

4.2.3. Limitations of the potentiostatic circuitry

In MET, electrolyte, membranes, electrodes, and microorganisms change their characteristics over time. This results in a variable current flow, complicating the analysis of individual components. The role of the potentiostat in a three-electrode electrochemical cell is to control the potential at the WE independently of changes at the electrodes and electrolyte. However, potentiostats can only compensate the resistance between the RE and CE within the voltage limitations or compliance voltage of the device, specifically based on the limitation of the PC amplifier [Figure 4]. Large WE can result in uneven electrode potential distribution, resulting in heterogenous biofilm growth and performance loss in MET (Oliot et al., 2017), therefore, small electrodes are preferable for analytical purposes.

Multiple potentiostats cannot be used to set different potentials to the same electrochemical cell at the same time, as this would cause interferences and affect the current readings. For such experimental configurations, modification of the original potentiostat circuits is required to set up a bipotentiostat or a multipotentiostat (Inzelt et al., 2013). These devices control one WE as previously explained [Figure 5C] and then additional WEs are referenced to the first one by an amplifier network (Bard and Faulkner, 2001).

Potentiostats typically use the same electrode to apply a potential and measure the resulting current. In electrochemical measurements such as conductivity, this could cause a polarization effect, due to

accumulation of charges, which can be avoided by implementing a four-electrode configuration (Schwan, 1968). In modern potentiostats, the same issue can be solved by using sense electrode probes for both WE and CE. A special technique, called electrochemical gating, is used to measure conductivity in potential-controlled conditions. Electrochemical gating relies on previous observations from semiconductor research, in which the charge stored in a certain material was shown to affect its conductivity (Chidsey and Murray, 1986). The typical configuration of an electrochemical gating experiment consists of maintaining a gate or threshold potential, which determines the charge storage status by the utilization of the potentiostatic control, and simultaneous measurement of the material conductivity [Figure 6]. In MET, this could be applied to study the conductivity of electroactive biofilms (Yates et al., 2018).

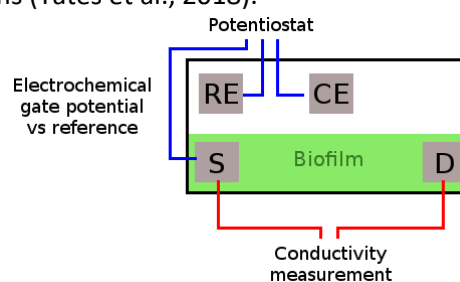


Figure 6: Electrochemical gating experiment with gate potential applied to the source (S) vs. the reference electrode (RE) and conductivity measurement between the source (S) and the drain (D). Modified from Vanmaekelbergh et al. (2007).

5. Polarization analyses for MET

5.1. Direct current techniques

5.1.1. Chronoamperometry and chronopotentiometry

Chronoamperometry (CA) consists on setting a fixed electrode potential at the WE against the RE while monitoring the current flow between WE and CE, whereas chronopotentiometry (CP) consists of controlling the current flow while monitoring the WE potential changes. In MET, long-term CA experiments are performed for culturing electroactive microorganisms and monitoring current exchange between the electrode and microorganisms for extended time periods (Batlle-Vilanova et al., 2017; Parameswaran et al., 2013). CP experiments have been less commonly applied to monitor the electrode potential when providing a constant electron flow to the microorganisms (Arends et al., 2017).

The optimal potential for electroactive microorganisms growth depends on the MET application, microorganisms involved in the process, electron transfer mechanisms (e. g. redox mediating molecules) and operational conditions (pH, substrate concentrations and temperature) (Costa et al., 2018; Dennis et al., 2016; Yang et al., 2012). Potentials

between -0.2 and 0.0 V vs. SHE are appropriate for growing anodic biofilms in MFCs (Chatterjee et al., 2019). Cathodic applications such as MES require a potential below the theoretical hydrogen evolution potential (-0.410 V vs. SHE at pH 7) (Rabaey and Rozendal, 2010).

5.1.2. Polarization sweep

Potential polarization sweep consists of monitoring the current response of an electrochemical cell when varying the WE electrode potential over a specific range, with a relatively slow scan rate, to achieve electrochemical equilibrium at each potential (pseudo steady-state). When such pseudo steady-state is achieved, the current flow at each potential is limited by the slowest reaction of the electron transfer chain (Bard and Faulkner, 2001). Thus, this technique allows to distinguish between different types of losses, namely activation, ohmic and concentration losses, based on the distinctive shape of the current vs. potential curve (i.e. polarization curve) [Figure 7A].

A typical polarization curve can be divided into three regions, referred as activation, ohmic and concentration polarization regions, which provide information on the main losses in the electrochemical cell under study. Activation losses represent the energy required for activating the oxidation/reduction reactions at the electrode surface. Ohmic losses are due to a set of resistances, including wiring (external resistance, current collectors and contacts) and ions transferred through the cell (electrolyte and membrane, if present). Concentration losses are associated to the transport of molecules to or from the electrode (Logan et al., 2006). Potential polarization sweeps can also be used to produce current vs. power plots, called power curves [Figure 7B]. Power curves are generally used to determine the maximum power attainable, e.g. when designing power sources. A power curve is typically parabolic in shape with a maximum power point (MPP), also called cell design point (CDP) (Logan et al., 2006; Saba et al., 2017).

Power and polarization curves are obtained using a potentiostat in two-electrode configuration, or by switching stepwise an external load (e.g. using a decade box changing resistor) at regular intervals from the open circuit potential (OCP) to a few Ω , and monitoring the whole cell potential response. The current is then calculated as the whole-cell potential divided by the resistance applied at each interval, according to Ohm's law. In MFCs, due to the presence of microorganisms, a stabilization period between 20 and 30 minutes is necessary at each resistance applied to attain stable potential measurements (Logan et al., 2006), although faster scan rates have also been proposed (Ieropoulos et al., 2010; Zhang et al., 2011).

The time allowed between resistance switches can affect the concentration of reactants, the electrode potential and the catalytic activity of microorganisms, and thus, the reproducibility of the measurements (Zhao et al., 2009).

Polarization curves can generate anomalous results due to power overshoot [Figure 7C], which results in a large voltage drop when applying high currents. It can be caused by electron transfer limitations, or to proton accumulation inside the cells (Nien et al., 2011; Watson and Logan, 2011). A precise control of the scan rate, using programmable specialized electronics such as a source measurement unit (SMU) or a potentiostat (Logan et al., 2006; Logan and Regan, 2006; Zhao et al., 2009), helps to avoid power overshoot. Polarization curves can be obtained, using a potentiostat, by continuously switching the applied potential, with a scan rate of 0.1 or 0.5 mV s⁻¹ (Arends et al., 2012; Ewing et al., 2014). Alternatively, the potential can be changed stepwise in a differential step voltammetry (DSV) or staircase voltammetry experiment. DSV reduces the interference from noise-producing capacitive currents, and amplifies the signal from chemical transformations (Faradaic processes) (Harnisch et al., 2012).

The potential of each electrode can be measured independently (against a RE) in an MFC while performing polarization curves. This helps detecting which electrode is limiting power production in the MFC, since the potential of the limiting electrode will change rapidly at high current values [Figure 7D], although it does not give information on the causes. An estimation of the causes for power losses can be, nevertheless, obtained by the current interrupt technique, consisting of interrupting the current flow and monitoring the potential change at each electrode (vs. RE) until it reaches the OCP. Ohmic losses correspond to the instantaneous potential change, whereas activation losses are associated with slower potential recovery [Figure 7E]. Current interrupt experiments, however, require a very fast data acquisition system capable of recording voltage values every 10 μ s or faster (Zhao et al., 2009).

5.1.3. Linear sweep and cyclic voltammetry

Several potentiostatic techniques, usually in three-electrode set-ups, are used in MET to characterize the catalytic effect of microorganisms on electrochemical reactions. Linear sweep voltammetry (LSV), where the WE potential is varied linearly vs. RE, can be used to measure the current flow between WE and CE as a function of the potential applied. LSV results can be shown as current vs. potential curves, similar to polarization curves, or as the logarithm of the current vs. overpotential [Tafel plots, Figure 7F]. Tafel plots

have been used to study electrode coatings (Ammar et al., 2018) as well as the catalytic capability of electroactive biofilms over time (Pous et al., 2013; Venkata Mohan et al., 2013).

Tafel plots show the equilibrium potential at the surface of the electrode in which the oxidation current equals the reduction current, and monitoring this potential over time gives information on the electrochemical reactions occurring at the electrode at each experiment stage (Srikanth and Venkata Mohan, 2012). Furthermore, Tafel plot slopes provide an estimation of the number of electrons transferred (based on the limiting electrochemical reaction) at the reducing or oxidizing potential applied [Figure 7F]. In combination with chemical analysis, Tafel plots can be used to study microbial-electrode interactions (Pous et al., 2013), which are often the limiting step in MET. However, similarly to polarization curves, the scan rate applied can affect the results.

Cyclic voltammetry (CV) is a widely used technique in MET research to investigate the electron transfer mechanisms, as well as to evaluate new electrode materials [Table 1]. CV is similar to LSV, but the potential is increased and decreased cyclically (forward and reverse scan) from two set potentials [Figure 8A] (Elgrishi et al., 2018). The voltage range applied in CVs for MET experiments is usually in the range of ± 1 V [Table 1], and strictly depends on the aim of the experiment. Relatively low-speed scan rates, between 1 and 50 mV s^{-1} [Table 1], are used for CV in MET due to the slow reaction rates of the biological reactions

(Harnisch et al., 2012). However, the optimal scan rate is case-specific, being dependent on the interactions between microorganisms, electrode surface/material and substrate type/concentration, and can only be determined experimentally. In CVs, redox-active molecules appear as peaks in the I-V plot [Figure 8B], and can thus be detected and quantified. If the redox reactions are electrochemically reversible, a peak will appear in both the forward and the reverse CV scan, and the potential value equidistant from the two peaks, called mid-point potential, will give information on the redox potential of the compound [Figure 8B]. Control CV experiments with a bare electrode (before colonization by microorganisms) are necessary for a correct interpretation of the results.

In MET, CVs can be applied in the presence (turnover CV) or absence (non-turnover CV) of substrate. CVs recorded under turnover conditions allow to study microbial growth at the electrode and to retrieve information on the catalytic activity and reaction rate limitations (Harnisch et al., 2012). Plotting the first derivative of the CV curve can improve visualisation of the redox peaks [Figure 8C]. CVs recorded under non-turnover conditions give information on the redox molecules mediating electron transfer between electroactive microorganisms and the electrode [Figure 8D]. However, achieving non-turnover conditions requires microbial starvation, which can cause microbial detachment from the electrode (Harnisch et al., 2012).

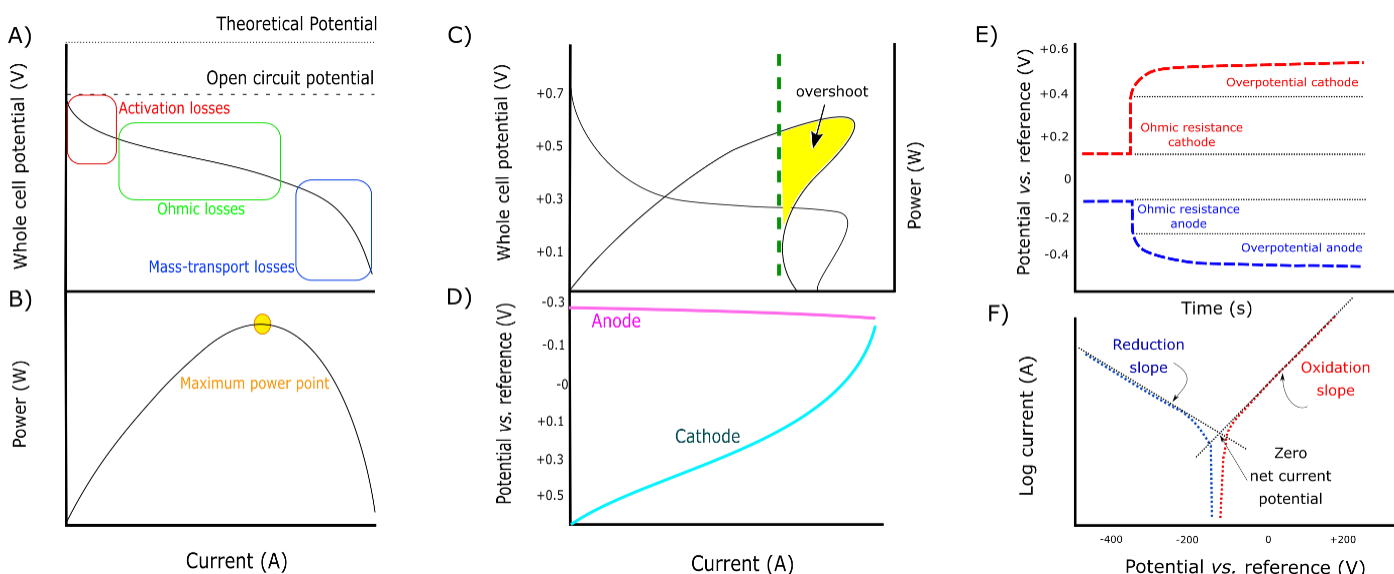


Figure 7: Potential vs. current polarization curve [A] and the corresponding power curve [B]. Power overshoot [C] common in power curves using fast sweeps. The anode and cathode potential [D] can be monitored during polarization experiments to understand system limitations. Current interrupt technique [E] showing the change in potential for the anode and cathode independently after the MFC current flow is stopped. Tafel plot showing reduction and oxidation slopes for WE in a three-electrode system [F].

Likewise polarization analysis, high speed scan rates are not appropriate for estimation of microbial electrocatalysis due to the relatively low reaction rates in microbial biofilms [Figure 8E], and can even damage the electroactive microorganisms. Further details on the electron transfer mechanisms can be obtained by studying the correlation between the scan rate and peak current [Figure 8F] (Harnisch et al., 2012). A

directly proportional relationship between scan rate and current peak reveals the presence of electroactive, adsorbed redox molecules typical of biofilms, whereas a linear relation between the square root of the scan rate and the peak current suggests electron transfer via soluble mediators (Babauta et al., 2012; Harnisch et al., 2012) or limited by diffusion within the biofilm.

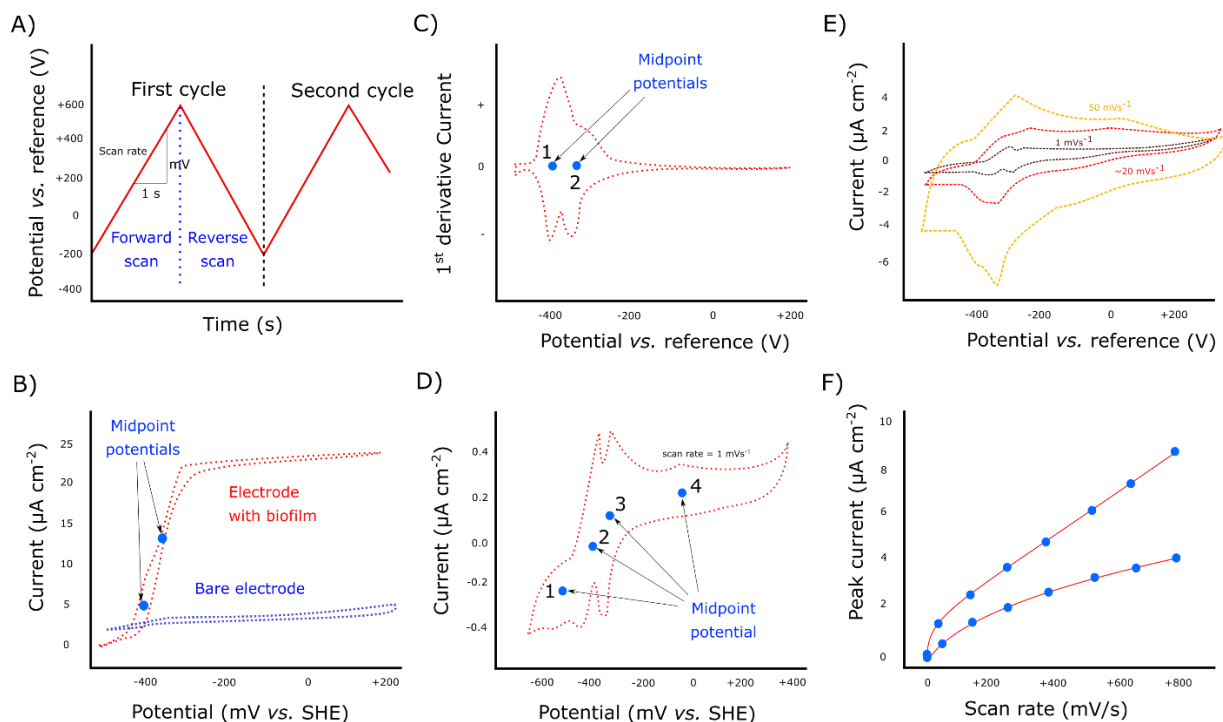


Figure 8: Typical polarization sweep sequence used for CV experiments [A]. CV with bare electrode and presence of biofilm showing the midpoint potentials [B]. First derivative analysis of the previous CV results which improves visualization of midpoint potentials [C]. Non-turnover CV which identifies 4 different redox components within the biofilm [D]. Non-turnover CV at different scan rates [E]. Scan rate vs. peak current plot to distinguish different electron transfer mechanisms (biofilm vs. planktonic) [F]. Example plots based on published work by Fricke et al. (2008).

Table 1: Cyclic voltammetry set-up for MET applications with different purposes, including potentiostat type, electrodes material, voltage range, and scan rate.

MET Type ^a	Aim of the study	Potentiostat (Brand, model)	Electrodes (WE, CE, RE)	WE Area (cm ²)	Voltage range (mV around RE)	Scan rate (mV/s)	Reference
MFC	Electricity production from starch processing wastewater by mixed culture	Autolab PGSTAT 30	WE: Carbon paper CE: Carbon paper with Pt catalyst RE: Ag/AgCl	25	-600 to 600	10	Lu et al., 2009
MFC	Study direct electron transfer from <i>Shewanella putrefaciens</i>	BAS CV-50W	WE: Glassy carbon CE: Pt RE: Ag/AgCl	0.07	-700 to 700	100	Kim et al., 2002
MFC	Electricity generation from artificial wastewater in upflow MFC	CH instruments 601B	WE: Glassy carbon CE: Pt RE: Ag/AgCl	0.07	-700 to 700	10, 30, 50 and 70	He et al., 2005
MFC	Testing a novel MFC and electrode design	BAS CV-50W	WE: Neutral red woven graphite felt CE: Porcelain-coated graphite felt RE: Ag/AgCl	0.07	-900 to 0	25	Park and Zeikus, 2003
MFC	Study electron transfer by <i>Geobacter sulfurreducens</i>	Autolab PGSTAT 30	WE: Graphite CE: Pt wire or carbon rod RE: Ag/AgCl	Not specified	-500 to 200 and -650 to 600	1, 5 and 50	Fricke et al., 2008
MFC	Comparison of the electron transfer from wild type vs. mutant <i>Geobacter sulfurreducens</i>	AMEL Instruments Model 2053	WE: Carbon cloth CE: Carbon cloth RE: Ag/AgCl	0.81 (equivalent to 2.4 cm ² plane graphite)	-500 to 300	From 2 to 5000	Richter et al., 2009
MFC	Study electron transfer by <i>Clostridium butyricum</i>	BAS CV-50W	WE: Glassy carbon CE: Pt RE: Ag/AgCl	0.13	-700 to 700	100	Park et al., 2001
MFC	Testing novel anode material	CHI660C	WE: Graphene (5 mg) coated stainless steel mesh CE: Carbon paper RE: Ag/AgCl	1	-800 to 400	10	Zhang et al., 2011
MFC	Testing novel anode material	Zahner-Elektrik IM6e	WE: Polypyrrole carbon nanotubes (17 mg) coated carbon paper CE: Platinum wire RE: Ag/AgCl	3.5	-1.0 to 1.0	50	Zou et al., 2008
MEC	Conversion of acidogenic effluents to hydrogen	Autolab PGSTAT12	WE (anode): Graphite plate CE: Graphite plate RE: Ag/AgCl	70	-0.5 to 0.5	30	Babu et al., 2013
MEC	Testing a novel biocathode for electromethanogenesis	Hokuto Denko HB-305	WE (cathode): Graphite felt fixed in carbon stick CE: Pt RE: Ag/AgCl	11	-1.4 to -0.4	5	Zhen et al., 2016
MEC	Optimize stainless steel mesh cathodes for hydrogen production	Gamry Instruments model PC4/750	WE (cathode): stainless steel CE: Pt plate RE: Ag/AgCl	7 to 24	-0.3 to 1.2	50	Zhang et al., 2010
MEC	Evaluate stainless steel and nickel alloys as cathode for hydrogen production	Gamry Instruments model PC4/750	WE (cathode): Stainless steel or nickel alloys CE: Graphite brush RE: Ag/AgCl	2200	0 to 1.0	1	Selembo et al., 2009
MEC	Evaluate methane production in an AD-MEC coupled system	Not applicable (Power supply + data logger)	WE (cathode): carbon felt CE: Stainless steel	25	-500 to 400	5	Yin et al., 2015

			RE: Ag/AgCl				
MES	Production of acetic acid from CO ₂	Biologic VMP3	WE (cathode): graphite rod and graphite granules CE: Graphite granules RE: Ag/AgCl	11 (rod) + granules	-200 to -1000 (vs. SHE)	1	Marshall et al., 2012
MES	Production of butyrate and isopropanol from CO ₂	Biologic VSP	WE (cathode): Carbon felt with stainless steel frame CE: Ti mesh RE: Ag/AgCl	100	-1400 to 0	1	Arends et al., 2017
MES	Evaluate long-term operation of electrosynthesis systems	Biologic VMP3	WE (cathode): Carbon rod and graphite granules CE: Carbon rod RE: Ag/AgCl	10 (rod) + granules	-1000 to -200 (vs. SHE)	1	Marshall et al., 2013
MES	Acetate production from CO ₂	Biologic VMP3	WE: Carbon felt CE: Titanium coated TaO ₂ /IrO ₂ mesh RE: Ag/AgCl	4	-1200 to 0	1	Patil et al., 2015
MES	Production of butyrate from CO ₂	Biologic SP50	WE: Carbon cloth CE: Ti rod RE: Ag/AgCl	9	-800 to 0	1	Ganigue et al., 2015

^a MFC = microbial fuel cell, MEC = microbial electrolysis cell, MES = microbial electrosynthesis

5.2. Alternating current techniques

5.2.1. The concept of impedance

The techniques described in the previous section are based on direct current (DC) measurements. Although CV analysis are performed by altering the current direction, due to the relatively slow transient period, it can be considered composed of two DC experiments, rather than an alternating current (AC) experiment. DC techniques have limitations deriving from the electrode polarization, which modifies the concentration of electroactive species around the electrode due to charge attraction and diffusion limitations. Furthermore, DC experiments can be inappropriate for the study of fundamental properties of the material, such as electrode capacitance or electrolyte conductivity.

In conductivity measurements, an AC square wave at an optimal frequency is applied between the electrodes to determine the resistance of the electrolyte, according to the Ohm's law, avoiding electrode polarization (Chidsey and Murray, 1986). However, when the system response depends on the AC wave frequency, not only the electrolyte resistance, but also its capacitance and induction component, ignored by the Ohm's law, play a role, and the concept of impedance must be introduced. Impedance (or reactance) is the frequency-dependent opposition of an element to the flow of current. The impedance of a system can be measured by applying sinusoidal AC excitation waves at different frequencies and measuring the resulting current response. This can be represented by Lissajous curves, where the amplitude and phase shift of the current response give an insight in the linear (resistive) and the non-linear (capacitive - inductive) component of the impedance, respectively. Impedance is fundamental to understand power transfer within electrical systems. MFCs, for example, can be considered as power sources with an intrinsic impedance or internal resistance, and power production is related to the impedance of the MFC device. A higher power density is typically attained in miniaturized MFCs due to the lower impedance (Choi, 2015; ElMekawy et al., 2013), but scaled up MFCs are required for real-world applications. Combination of MET with other technological solutions, such as energy harvesters (Carreon-Bautista et al., 2015) and supercapacitors, is a potential solution to mitigate the power limitations of MFCs (Dubal et al., 2015). However, implementation of such systems requires an in-depth understanding of impedance.

5.2.3. Electrochemical impedance spectroscopy

The electrochemical impedance spectroscopy (EIS) technique is used to study the response of an electrochemical system to potential waves at different

AC frequencies. EIS has been widely used in the last 10 years in MET research, mainly to test novel electrode materials and configurations, and their interaction with microorganisms [Table 2]. EIS is performed by a potentiostat equipped with an additional frequency analysis module. A sinusoidal AC wave is applied at the summing point (Sum) of the PC amplifier [Figure 4] resulting in an oscillating WE potential around the set potential for which the current response is analysed. In MET research, AC wave amplitudes between 1 and 10 mV are usually applied in EIS experiments to produce a linear response from the system [Table 2], since wider amplitudes increase the risk of producing a non-linear response that further complicate the analysis. EIS analysis in MET is usually performed over a wide range of frequencies from a few mHz to 100 kHz or 1 MHz [Table 2].

When several AC sinusoidal waves are used, mathematical functions such as the Fourier transform are required to simplify the information contained on the excitation and response signals. Each sinusoid with constant amplitude and frequency can be simplified to a vector in which the modulus represents the amplitude and the angle represents the initial phase, to obtain a phasor diagram of the signal by the rotating vector method (Bard and Faulkner, 2001). The phasor diagram can thus represent the system's response to the excitation wave through a vector indicating the change in the real (resistance) and imaginary (reactance) part.

EIS results are typically plotted as Bode plots, which give explicit information on the relation between the AC wave excitation frequency and the amplitude and phase of the response [Figure 9A], and Nyquist plots, in which results are represented in the condensed form in the complex plane [Figure 9B]. Nyquist plots allow to directly extract certain parameters from the shape of the curve, as the electrolyte resistance (R_s) and charge transfer resistances (R_{ct}) correspond to the intersection of the curve to the real-part axis [Figure 9B].

Table 2: Electrochemical impedance spectroscopy set-up for MET applications with different purposes, including potentiostat type, electrodes material, equivalent circuits proposed, frequency range and AC signal amplitude applied.

MET Type ^a	Aim of the study	Potentiostat (Brand, model)	Electrodes (WE, CE, RE)	WE Area (cm ²)	Equivalent circuit ^b	Frequency range	AC signal amplitude	Reference
MFC	Study a novel anode material	Autolab PGSTAT30	WE (anode): Carbon nanotube/polyaniline composite CE: Pt RE: Saturated Calomel	1		500 mHz to 100 kHz	10 mV	Qiao et al., 2007
MFC	Study a novel cathode	CHI 660D	WE (cathode): Activated carbon/PTFE composite CE: Pt sheet RE: Ag/AgCl	7		10 mHz to 100 kHz	10 mV	Dong et al., 2012
MFC	Study a novel anode material	CHI 660D	WE (anode): Graphene/Polyaniline nanocomplex modified carbon cloth CE: Carbon felt RE: Ag/AgCl	3.24		5 mHz to 100 kHz	10 mV	Hou et al., 2013
MFC	Study the effect of applied potential on impedance	AMETEK-AMT	WE (anode): Plain graphite CE: Plain graphite RE: Ag/AgCl	50 (anode) 50 (cathode)		10 mHz to 100 kHz	n.a.	Wang et al., 2009
MFC	Determine electrochemical properties of MFCs	Gamry PCI4/300	WE (anode): Bare graphite CE: Graphite with Pt RE: Ag/AgCl	20	Not specified	1 mHz to 100 kHz	10 mV	Manohar et al., 2008
MFC	Study the impact of biofilm on MFC impedance	Zahner™ IM6ex	WE (cathode): Microfibrous carbon paper CE: Microfibrous carbon paper RE: Ag/AgCl	15.2		100 mHz to 10 kHz	10 mV	Ramasamy et al., 2008
MFC	Compare anode configurations	IVIUMStat	WE (anode): flat graphite, Al ₂ O ₃ -blasted graphite, Pt-coated Ti or uncoated Ti CE: Flat graphite plate RE: Ag/AgCl	22		3 mHz to 40 Hz	n.a.	ter Heijne et al., 2008
MFC	Test a novel anode configuration	PAR 283	WE (anode): Carbon nanotube CE: Platinum coated carbon paper RE: Cathode electrode	15		5 mHz to 100 kHz	10 mV	Sun et al., 2010


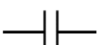
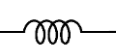
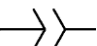
MFC	Test a tubular MFC with membrane electrode assembly cathode	Solartron Analytical	WE (cathode): Pt containing carbon cloth CE: Activated carbon RE: Ag/AgCl	>100		1 mHz to 300 kHz	15 mV	Kim et al., 2009
MFC	Test a novel air-cathode	Parstat 263A	WE (anode): Graphite granules CE: Pt coated carbon cloth RE: None	31		10 mHz to 100 kHz	10 mV	You et al., 2007
MDS	Evaluate start-up of a biocathode MDS	CHI 660	WE (anode): Graphite brush CE: Graphite brush and granules RE: Ag/AgCl	5560		10 mHz to 100 kHz	5 mV	Meng et al., 2014
MEC	Anode arrangement optimization	Parstat 2273	WE (anode): Graphite felt CE: Carbon cloth RE: Saturated calomel	> 28		10 mHz to 100 kHz	10 mV	Liang et al., 2011
MEC	Study the effect of a sulphate reducing bacteria biofilm on electron transfer rate	Autolab PGSTAT302N	WE (anode): Graphite rod CE: Graphite rod RE: Ag/AgCl	44		10 Hz to 100 kHz	5 mV	Wang et al., 2017
MEC	Study the effect of applied voltage of methane production	Versastat 3	WE (cathode): Carbon fiber brush with stainless steel wire CE: Carbon fiber brush RE: Ag/AgCl	41 (approx. by solid cylinder)	Not specified	10 mHz to 1000 kHz	10 mV	Choi et al., 2017

^a MFC = microbial fuel cell; MEC = microbial electrolysis cell; MES = microbial electrosynthesis.

^b R_s = Solution resistance, R_{CT} = Charge transfer resistance, R_{POLZ} = Polarization resistance, R_{IN} = Contact or interphase resistance, C_{DL} = double layer capacitance, C_{AD} = Adsorption capacitance, W = Warburg element modelling the diffusion process, CPE = Constant phase element, L = Inductance.

A more detailed impedance analysis can be obtained by postulating an electrical circuit (equivalent circuit) in which electrical components with known impedance, such as resistors, inductors, and capacitors [Table 3] simulate the physical, chemical and biological processes occurring in the MET device. The Randles model [Figure 9C], including electrode capacitance (C_{dl}), electrolyte and charge transfer resistances (R_S and R_{ct}) and diffusion limitations, represented by a Warburg element (W), is typically used in MET to represent the electrochemical reactions occurring at one electrode. Fitting the experimental data to a meaningful equivalent circuit, representing the electrochemical set-up under analysis, by means of computer algorithms (e.g. non-linear least squares, NLLS), allows quantifying the impedance values of each of the components of the circuit. Different equivalent circuits have been proposed based on the MET design, which could be divided into single electrode and whole electrochemical cell models [Table 2]. While single-electrode models help understanding the reactions and the nature of electron transfer in (bio)electrochemical systems, whole electrochemical cell models are suitable to determine the limiting factors of the electrochemical systems, including the impedance of the elements present between the electrodes (membrane and electrolyte).

Table 3: Different electric circuit elements and electrochemical abstractions with their impedance formula.

Impedance element	Symbol	Impedance formula	Explanation
Resistor		R	Impedance correspond to the resistance in ohms (R)
Capacitor		$-1/j\omega C$	Impedance inversely proportional to the angular frequency (ω) and the capacitance (C)
Inductor		$j\omega L$	Impedance proportional to the angular frequency (ω) and the inductance (L)
Constant phase element (CPE)		$1/Q_0(j\omega)^\alpha$	CPE model the behaviour of the double layer as an imperfect capacitor and admittance value (Q). CPE can define non-homogenous electrochemical reactions on the surface of the electrode.
Warburg element	W	$1/Q_0(j\omega)^{1/2}$	Special type of CPE in which the phase is independent of frequency and equals 45 degrees. It often reflects diffusion limitations.

To ensure the quality of the electrochemical analysis, the response to the applied AC waves must be solely due to the excitation signals applied avoiding interferences from distortions of the AC wave or from unstable systems. However, it is challenging to achieve

stability in dynamic biological systems such as MET (Dominguez-Benetton et al., 2012), as microorganism-based systems are continuously changing. Emerging or innovative methods that avoid stepwise change of excitation AC wavelengths, as those with multiple simultaneous sin waves, or white noise excitation and posterior signal deconvolution, might be useful to shorten the experiment time and thus reduce the effect of EIS analysis on biological structures (Barsoukov and Macdonald, 2005; Chang and Park, 2010).

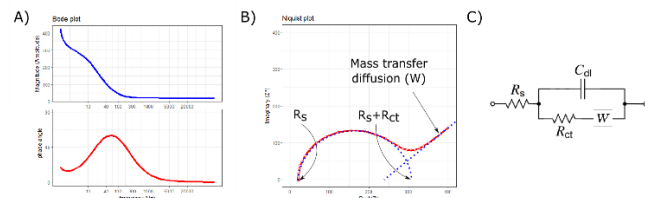


Figure 9: Bode plot for the phase and modulus of the response to different excitation frequencies [A]. Nyquist plot [B] with graphical representation of ohmic resistance (R_S), charge transfer resistance (R_{ct}), and mass transfer diffusion resistance (W). Randles circuit [C] showing the typical elements that model the electrode interface. The Bode and Nyquist plots were obtained by performing a simulation of a Randles circuit with electrolyte resistance (R_S) of 20 Ω , charge transfer resistance (R_{ct}) of 250 Ω , double layer capacitance (C_{dl}) of 40 μF and Warburg element (W) of 150 Ωs^{-1} with R programming software according to the formulas in Table 3.

6. Future perspectives for electronics in MET

Due to the broad range of configurations, METs require different types of electronic devices to control and understand the microbial electrochemical reactions. However, the lack of standardization of the tools and protocols in MET research is hampering the development of the field. Furthermore, knowledge on electronic concepts is necessary to design experimental set-ups and retrieve information from the results. Understanding the electronic circuits, being able to tweak their capabilities and programming them, will further boost MET research.

The potentiostat is a fundamental electrochemical tool for MET research, but the commercial ones are not economically affordable for many research groups. Low-cost potentiostat devices, including open-source potentiostat devices, have recently been proposed (Dobbelaere et al., 2017; Dryden and Wheeler, 2015; Rowe et al., 2011). The development of open-source devices can provide the necessary infrastructure for MET experiments at low cost, allowing to perform experiments with the necessary replicates, which are often omitted in MET research due to the high costs of bioreactors and instruments. The establishment of open-source potentiostats would also improve comparison between different research groups and experiments, which remains an important limitation for MET development (Koch and Harnisch, 2016).

Furthermore, combining potentiostatic devices with more energetically efficient amplification than the common AB push-pull amplifiers, such as the D-type energy amplifiers (Habibi et al., 2010), can facilitate MET applications by reducing the energy requirements of potentiostatic control.

Open-source opens a new paradigm for licensing technologies which allows continuous and distributed development of the devices. For example, the development of the DStat open-source potentiostat (Dryden and Wheeler, 2015) provided a base upon which a new open source potentiostat with added EIS functionality and wireless connectivity was implemented (Jenkins et al., 2019). Open source licensing can boost MET research and application, as it may bridge the gap between MET researchers and application industries, favouring commercialization of MET (Dryden et al., 2017; Pearce, 2017).

7. Conclusions

METs are biological systems that require control and measurement of electrical and electrochemical parameters. However, the electronic devices required for MET analysis are often black boxes for MET researchers, and the lack of background on electronics, including analytical devices and their limitations, can cause misleading experimental results, especially in the case of using large surface electrodes. This review provides a comprehensive overview of the electronic background necessary to understand and perform

electrochemical analysis on MET, common values used for the parameters and what information can be retrieved from the data. Understanding the electronics behind MET will lead to more effective experimental designs and promote standardization across the field. Open source hardware can contribute to understand the electronic limitations and capabilities of the laboratory infrastructure and promote developing tailored MET solutions while reducing the cost of access to these technologies in laboratories with low economic resources. The versatility offered by microbial electrochemistry has potential to improve chemical transformation processes in waste remediation and biofuels research. Joining the gap between electronics and microbiology is the most logical step to move METs towards their maturity and promote their application and commercialization within the environmental engineering sector.

8. Acknowledgements

This work has been financed by the Science Foundation Ireland (SFI) Research Professorship Programme *Innovative Energy Technologies for Biofuels, Bioenergy and a Sustainable Irish Bioeconomy* (award no. 15/RP/2763). The authors thank Uwe Schröder group (Technische Universität Braunschweig, Germany) for kindly permitting re-using their data to plot the graphs shown on Figure 8.

References

- Ammar, A.U., Shahid, M., Ahmed, M.K., Khan, M., Khalid, A., Khan, Z.A., 2018. Electrochemical study of polymer and ceramic-based nanocomposite coatings for corrosion protection of cast iron pipeline. *Materials (Basel)*. 9, 332. <https://doi.org/10.3390/ma11030332>
- Arends, J.B.A., Blondeel, E., Tennison, S.R., Boon, N., Verstraete, W., 2012. Suitability of granular carbon as an anode material for sediment microbial fuel cells. *J. Soils Sediments* 12, 1197–1206. <https://doi.org/10.1007/s11368-012-0537-6>
- Arends, J.B.A.A., Patil, S.A., Roume, H., Rabaey, K., 2017. Continuous long-term electricity-driven bioproduction of carboxylates and isopropanol from CO₂ with a mixed microbial community. *J. CO₂ Util.* 20, 141–149. <https://doi.org/10.1016/j.jcou.2017.04.014>
- Babauta, J., Renslow, R., Lewandowski, Z., Beyenal, H., 2012. Electrochemically active biofilms: Facts and fiction. A review. *Biofouling* 28, 789–812. <https://doi.org/10.1080/08927014.2012.710324>
- Bard, A.J., Faulkner, L.R., 2001. *Electrochemical Methods: Fundamentals and Applications*, 2nd ed. JOHN WILEY SONS INC. <https://doi.org/10.1016/B978-0-12-381373-2.00056-9>
- Barsoukov, E., Macdonald, J.R., 2005. *Impedance Spectroscopy; Theory, Experiment, and Applications*, 2nd ed. Wiley Interscience Publications. <https://doi.org/10.1002/0471716243.fmatter>
- Batlle-Vilanova, P., Ganigué, R., Ramió-Pujol, S., Bañeras, L., Jiménez, G., Hidalgo, M., Balaguer, M.D., Colprim, J., Puig, S., 2017. Microbial electrosynthesis of butyrate from carbon dioxide: Production and extraction. *Bioelectrochemistry* 117, 57–64. <https://doi.org/10.1016/j.bioelechem.2017.06.004>
- Bio-Logic, 2015. How to read EIS accuracy contour plots. *Appl. notes* 54, 1–5.
- Bond, D.R., 2007. Chapter 93: Growth of electrode-reducing bacteria, 3rd ed. ed, *Manual of environmental microbiology*. ASM press, Washington, DC. <https://doi.org/10.1128/9781555815882.ch93>
- Borjas, Z., Esteve-Núñez, A., Ortiz, J.M., 2017. Strategies for merging microbial fuel cell technologies in water desalination processes: Start-up protocol and desalination efficiency assessment. *J. Power Sources* 356, 519–528.
- Bruce, J.H., Hickling, A., 1937. A current stabiliser for electrolytic circuits. *J. Sci. Instrum.* 14, 367–370. <https://doi.org/10.1088/0950-7671/14/11/303>
- Busoni, L., Carlà, M., Lanzi, L., 2002. A comparison between potentiostatic circuits with grounded work or auxiliary electrode. *Rev. Sci. Instrum.* 73, 1921–1923. <https://doi.org/10.1063/1.1463715>
- Carreon-Bautista, S., Erbay, C., Han, A., Sánchez-Sinencio, E., 2015. Power management system with integrated maximum power extraction algorithm for microbial fuel cells. *IEEE Trans. Energy Convers.* 30, 262–272. <https://doi.org/10.1109/TEC.2014.2352654>
- Chang, B.-Y., Park, S.-M., 2010. Electrochemical Impedance Spectroscopy. *Annu. Rev. Anal. Chem.* 3, 207–229. <https://doi.org/10.1146/annurev.anchem.012809.102211>
- Chatterjee, P., Dessì, P., Kokko, M., Lakaniemi, A.-M., Lens, P., 2019. Selective enrichment of biocatalysts for bioelectrochemical systems: A critical review. *Renew. Sustain. Energy Rev.* 109, 10–23. <https://doi.org/10.1016/J.RSER.2019.04.012>
- Chidsey, C.E.D., Murray, R.W., 1986. Redox capacity and direct current electron conductivity in electroactive materials. *J. Phys. Chem.* 90, 1479–1484.
- Choi, K.S., Kondaveeti, S., Min, B., 2017. Bioelectrochemical methane (CH₄) production in anaerobic digestion at different supplemental voltages. *Bioresour. Technol.* 245, 826–832. <https://doi.org/10.1016/j.biortech.2017.09.057>
- Choi, S., 2015. Microscale microbial fuel cells: Advances and challenges. *Biosens. Bioelectron.* 69, 8–25. <https://doi.org/10.1016/j.bios.2015.02.021>
- Costa, N.L., Clarke, T.A., Philipp, L.-A.A., Gescher, J., Louro, R.O., Paquete, C.M., 2018. Electron transfer process in microbial electrochemical technologies: The role of cell-surface exposed conductive proteins. *Bioresour. Technol.* 255, 308–317. <https://doi.org/10.1016/j.biortech.2018.01.133>
- Dennis, P.G., Viridis, B., Vanwonterghem, I., Hassan, A., Hugenholtz, P., Tyson, G.W., Rabaey, K., 2016. Anode potential influences the structure and function of anodic electrode and electrolyte-associated microbiomes. *Sci. Rep.* 6, 1–11. <https://doi.org/10.1038/srep39114>
- Dobbelaere, T., Vereecken, P.M., Detavernier, C., 2017. A USB-controlled potentiostat/galvanostat for thin-film battery characterization. *HardwareX* 2, 34–49. <https://doi.org/10.1016/j.ohx.2017.08.001>
- Doelling, R., 2000. Potentiostats: An introduction to the principle of potentiostatic control, including basic

potentiostatic circuits, electrochemical applications, and some notes on electrode and cell design.

- Doelling, R., 1998. Hans Wenking, born August 18th, 1923 A problem-solver for electrochemists. *Mater. Corros.* 49, 535–538.
- Dominguez-Benetton, X., Sevda, S., Vanbroekhoven, K., Pant, D., Vanbroekhoven, K., Pant, D., Vanbroekhoven, K., Pant, D., 2012. The accurate use of impedance analysis for the study of microbial electrochemical systems. *Chem. Soc. Rev.* 41, 7228–7246. <https://doi.org/10.1039/c2cs35026b>
- Dong, H., Yu, H., Wang, X., Zhou, Q., Feng, J., 2012. A novel structure of scalable air-cathode without Nafion and Pt by rolling activated carbon and PTFE as catalyst layer in microbial fuel cells. *Water Res.* 46, 5777–5787. <https://doi.org/10.1016/j.watres.2012.08.005>
- Dryden, M.D.M., Fobel, R., Fobel, C., Wheeler, A.R., 2017. Upon the shoulders of giants: open-source hardware and software in analytical chemistry. *Anal. Chem.* 89, 4330–4338. <https://doi.org/10.1021/acs.analchem.7b00485>
- Dryden, M.D.M.M., Wheeler, A.R., 2015. DStat: A versatile, open-source potentiostat for electroanalysis and integration. *PLoS One* 10, 1–17. <https://doi.org/10.1371/journal.pone.0140349>
- Dubal, D.P., Ayyad, O., Ruiz, V., Gómez-Romero, P., 2015. Hybrid energy storage: The merging of battery and supercapacitor chemistries. *Chem. Soc. Rev.* <https://doi.org/10.1039/c4cs00266k>
- Elgrishi, N., Rountree, K.J., McCarthy, B.D., Rountree, E.S., Eisenhart, T.T., Dempsey, J.L., 2018. A Practical Beginner's Guide to Cyclic Voltammetry. *J. Chem. Educ.* 95, 197–206. <https://doi.org/https://doi.org/10.1021/acs.jchemed.7b00361>
- ElMekawy, A., Hegab, H.M., Dominguez-Benetton, X., Pant, D., 2013. Internal resistance of microfluidic microbial fuel cell: Challenges and potential opportunities. *Bioresour. Technol.* 142, 672–682. <https://doi.org/10.1016/j.biortech.2013.05.061>
- Enke, C.G., 2015. The analog revolution and its on-going role in modern analytical measurements. *Anal. Chem.* <https://doi.org/10.1021/acs.analchem.5b02405>
- Ewing, T., Ha, P.T., Babauta, J.T., Tang, N.T., Heo, D., Beyenal, H., 2014. Scale-up of sediment microbial fuel cells. *J. Power Sources* 272, 311–319. <https://doi.org/10.1016/j.jpowsour.2014.08.070>
- Fangzhou, D., Zhenglong, L., Shaoqiang, Y., Beizhen, X., Hong, L., 2011. Electricity generation directly using human feces wastewater for life support system. *Acta Astronaut.* 68, 1537–1547.
- Franklin, B., 1751. Experiments and observations on electricity made in Philadelphia in America. Printed and sold by E. Cave at St. John's Gate.
- Fricke, K., Harnisch, F., Schröder, U., 2008. On the use of cyclic voltammetry for the study of anodic electron transfer in microbial fuel cells. *Energy Environ. Sci.* 1. <https://doi.org/10.1039/b802363h>
- Ganigue, R., Puig, S., Batlle-Vilanova, P., Balaguer, M.D., Colprim, J., 2015. Microbial electrosynthesis of butyrate from carbon dioxide. *Chem. Commun.* 51, 3235–3238.
- Habibi, M., Ghanbari, S., Mehdi Habibi, S.C., 2010. Application of class D power amplifiers in low power potentiostat circuits. *Int. J. Circuit Theory Appl.* 45, 790–810. <https://doi.org/10.1002/cta>
- Harnisch, F., Frequia, S., Freguia, S., Biofilms, M., 2012. A basic tutorial on cyclic voltammetry for the investigation of electroactive microbial biofilms. *Chem. an Asian J.* 7, 466–475. <https://doi.org/10.1002/ASIA.201100740>
- He, Z., Minteer, S.D., Angenent, L.T., 2005. Electricity generation from artificial wastewater using an upflow microbial fuel cell. *Environ. Sci. Technol.* 39, 5262–5267. <https://doi.org/10.1021/es0502876>
- Heyrovský, J., 1925. Researches with the dropping mercury cathode: Part I. General introduction. *Recl. des Trav. Chim. des Pays-Bas* 44, 488–495. <https://doi.org/10.1002/recl.19250440605>
- Hou, J., Liu, Z., Zhang, P., 2013. A new method for fabrication of graphene/polyaniline nanocomplex modified microbial fuel cell anodes. *J. Power Sources* 224, 139–144. <https://doi.org/10.1016/j.jpowsour.2012.09.091>
- Ieropoulos, I., Winfield, J., Greenman, J., 2010. Effects of flow-rate, inoculum and time on the internal resistance of microbial fuel cells. *Bioresour. Technol.* 101, 3520–3525. <https://doi.org/10.1016/j.biortech.2009.12.108>
- Inzelt, G., Lewenstam, A., Scholz, F., 2013. *Handbook of Reference Electrodes*. Springer. <https://doi.org/10.1007/978-3-642-36188-3>
- Jenkins, D.M., Lee, B.E., Jun, S., Reyes-De-Corcuera, J., McLamore, E.S., 2019. ABE-Stat, a fully open-source and versatile wireless potentiostat project including electrochemical impedance spectroscopy. *J. Electrochem. Soc.* 166, B3056–B3065. <https://doi.org/10.1149/2.0061909jes>
- Jiang, X., Hu, J., Petersen, E.R., Fitzgerald, L.A., Jackan, C.S., Lieber, A.M., Ringeisen, B.R., Lieber, C.M., Biffinger,

- J.C., 2013. Probing single- to multi-cell level charge transport in *Geobacter sulfurreducens* DL-1. *Nat. Commun.* 4, 2751. <https://doi.org/10.1038/ncomms3751>
- Khaled, F., Ondel, O., Allard, B., 2016. Microbial fuel cells as power supply of a low-power temperature sensor. *J. Power Sources* 306, 354–360. <https://doi.org/10.1016/J.JPOWSOUR.2015.12.040>
 - Kim, H.J., Park, H.S., Hyun, M.S., Chang, I.S., Kim, M., Kim, B.H., 2002. A mediator-less microbial fuel cell using a metal reducing bacterium, *Shewanella putrefaciens*. *Enzyme Microb. Technol.* 30, 145–152. [https://doi.org/10.1016/S0141-0229\(01\)00478-1](https://doi.org/10.1016/S0141-0229(01)00478-1)
 - Kim, J.R., Premier, G.C., Hawkes, F.R., Dinsdale, R.M., Guwy, A.J., 2009. Development of a tubular microbial fuel cell (MFC) employing a membrane electrode assembly cathode. *J. Power Sources* 187, 393–399. <https://doi.org/10.1016/j.jpowsour.2008.11.020>
 - Koch, C., Harnisch, F., 2016. What is the essence of microbial electroactivity? *Front. Microbiol.* 7, 1–5. <https://doi.org/10.3389/fmicb.2016.01890>
 - Ledoux, N., 2011. Technical Article MS-2256: Breaking Ground Loops with Functional Isolation to Reduce Data Transmission Errors.
 - Lenin Babu, M., Venkata Subhash, G., Sarma, P.N., Venkata Mohan, S., 2013. Bio-electrolytic conversion of acidogenic effluents to biohydrogen: An integration strategy for higher substrate conversion and product recovery. *Bioresour. Technol.* 133, 322–331. <https://doi.org/10.1016/j.biortech.2013.01.029>
 - Liang, D.W., Peng, S.K., Lu, S.F., Liu, Y.Y., Lan, F., Xiang, Y., 2011. Enhancement of hydrogen production in a single chamber microbial electrolysis cell through anode arrangement optimization. *Bioresour. Technol.* 102, 10881–10885. <https://doi.org/10.1016/j.biortech.2011.09.028>
 - Logan, B.E., Hamelers, B., Rozendal, R., Schröder, U., Keller, J., Freguia, S., Aelterman, P., Verstraete, W., Rabaey, K., 2006. Microbial fuel cells: Methodology and technology. *Environ. Sci. Technol.* 40, 5181–5192. <https://doi.org/10.1021/es0605016>
 - Logan, B.E., Regan, J.M., 2006. Electricity-producing bacterial communities in microbial fuel cells. *Trends Microbiol.* 14, 512–518. <https://doi.org/10.1016/j.tim.2006.10.003>
 - Lohner, S.T., Tiehm, A., 2009. Application of electrolysis to stimulate microbial reductive PCE dechlorination and oxidative VC biodegradation. *Environ. Sci. Technol.* 43, 7098–7104. <https://doi.org/10.1021/es900835d>
 - Lu, N., Zhou, S., Zhuang, L., Zhang, J., Ni, J., 2009. Electricity generation from starch processing wastewater using microbial fuel cell technology. *Biochem. Eng. J.* 43, 246–251. <https://doi.org/10.1016/j.bej.2008.10.005>
 - Ma, W.J., Luo, C.H., Lin, J.L., Chou, S.H., Chen, P.H., Syu, M.J., Kuo, S.H., Lai, S.C., 2016. A portable low-power acquisition system with a urease bioelectrochemical sensor for potentiometric detection of urea concentrations. *Sensors (Switzerland)* 16, 474. <https://doi.org/10.3390/s16040474>
 - Manohar, A.K., Bretschger, O., Neelson, K.H., Mansfeld, F., 2008. The use of electrochemical impedance spectroscopy (EIS) in the evaluation of the electrochemical properties of a microbial fuel cell. *Bioelectrochemistry* 72, 149–154. <https://doi.org/10.1016/j.bioelechem.2008.01.004>
 - Markoff, J., 2014. Andrew Kay, Pioneer in Computing, dies at 95.
 - Marshall, C.W., Ross, D.E., Fichot, E.B., Norman, R.S., May, H.D., 2013. Long-term operation of microbial electrosynthesis systems improves acetate production by autotrophic microbiomes. *Environ. Sci. Technol.* 47, 6023–6029. <https://doi.org/10.1021/es400341b>
 - Marshall, C.W., Ross, D.E., Fichot, E.B., Norman, R.S., May, H.D., 2012. Electrosynthesis of commodity chemicals by an autotrophic microbial community. *Appl. Environ. Microbiol.* 78, 8412–8420. <https://doi.org/10.1128/AEM.02401-12>
 - Meloni, G.N., 2016. Building a microcontroller based potentiostat: A inexpensive and versatile platform for teaching electrochemistry and instrumentation. *J. Chem. Educ.* 93, 1320–1322. <https://doi.org/10.1021/acs.jchemed.5b00961>
 - Meng, F., Jiang, J., Zhao, Q., Wang, K., Zhang, G., Fan, Q., Wei, L., Ding, J., Zheng, Z., 2014. Bioelectrochemical desalination and electricity generation in microbial desalination cell with dewatered sludge as fuel. *Bioresour. Technol.* 157, 120–126. <https://doi.org/10.1016/j.biortech.2014.01.056>
 - Morrison, R., 2016. *Grounding and Shielding: Circuits and interference*, 6th ed. JOHN WILEY SONS INC.
 - Nancharaiah, Y. V., Mohan, S.V., Lens, P.N.L., 2016. Biological and bioelectrochemical recovery of critical and scarce metals. *Trends Biotechnol.* 34, 137–155. <https://doi.org/10.1016/j.tibtech.2015.11.003>
 - Nevin, K.P., Woodard, T.L., Franks, A.E., Summers, Z.M., Lovley, D.R., 2010. Microbial electrosynthesis: feeding microbes electricity to convert carbon dioxide and water to multicarbon extracellular organic compounds. *MBio* 1, e00103-10. <https://doi.org/10.1128/mBio.00103-10>

- Nien, P.-C., Lee, C.-Y., Ho, K.-C., Adav, S.S., Liu, L., Wang, A., Ren, N., Duu-Jong Lee, 2011. Power overshoot in two-chambered microbial fuel cell (MFC). *Bioresour. Technol.* 102, 4742–4746.
- Olliot, M., Chong, P., Erable, B., Bergel, A., 2017. Influence of the electrode size on microbial anode performance. *Chem. Eng. J.* 327, 218–227. <https://doi.org/10.1016/j.cej.2017.06.044>
- Parameswaran, P., Bry, T., Popat, S.C., Lusk, B.G., Rittmann, B.E., Torres, C.I., 2013. Kinetic, electrochemical, and microscopic characterization of the thermophilic, anode-respiring bacterium *Thermincola ferriacetica*. *Environ. Sci. Technol.* 47, 4934–4940. <https://doi.org/10.1021/es400321c>
- Park, D.H., Zeikus, J.G., 2003. Improved fuel cell and electrode designs for producing electricity from microbial degradation. *Biotechnol. Bioeng.* 81, 348–355. <https://doi.org/10.1002/bit.10501>
- Park, H.S., Kim, B.H., Kim, H.S., Kim, H.J., Kim, G.T., Kim, M., Chang, I.S., Park, Y.K., Chang, H.I., 2001. A novel electrochemically active and Fe(III)-reducing bacterium phylogenetically related to *Clostridium butyricum* isolated from a microbial fuel cell. *Anaerobe* 7, 297–306. <https://doi.org/10.1006/ANAE.2001.0399>
- Patil, S.A., Arends, J.B.A., Vanwonterghem, I., Van Meerbergen, J., Guo, K., Tyson, G.W., Rabaey, K., 2015. Selective enrichment establishes a stable performing community for microbial electrosynthesis of acetate from CO₂. *Environ. Sci. Technol.* 49, 8833–8843. <https://doi.org/10.1021/es506149d>
- Pearce, J.M., 2017. Emerging business models for open source hardware. *J. Open Hardw.* 1, 1–14. <https://doi.org/10.5334/joh.4>
- Potter, M.C., 1911. Electrical effects accompanying the decomposition of organic compounds. *Proc. R. Soc. London. Ser. B Biol. Sci.* B, 260–276.
- Pous, N., Carmona-Martínez, A.A., Vilajeliu-Pons, A., Fiset, E., Bañeras, L., Trably, E., Balaguer, M.D., Colprim, J., Bernet, N., Puig, S., 2016. Bidirectional microbial electron transfer: Switching an acetate oxidizing biofilm to nitrate reducing conditions. *Biosens. Bioelectron.* 75, 352–358. <https://doi.org/10.1016/j.bios.2015.08.035>
- Pous, N., Puig, S., Coma, M., Balaguer, M.D., Colprim, J., 2013. Bioremediation of nitrate-polluted groundwater in a microbial fuel cell. *J. Chem. Technol. Biotechnol.* 88, 1690–1696. <https://doi.org/10.1002/jctb.4020>
- Qiao, Y., Li, C.M., Bao, S.J., Bao, Q.L., 2007. Carbon nanotube/polyaniline composite as anode material for microbial fuel cells. *J. Power Sources* 170, 79–84. <https://doi.org/10.1016/j.jpowsour.2007.03.048>
- Rabaey, K., Read, S.T., Clauwaert, P., Freguia, S., Bond, P.L., Blackall, L.L., Keller, J., 2008. Cathodic oxygen reduction catalyzed by bacteria in microbial fuel cells. *ISME J.* 2, 519–527. <https://doi.org/10.1038/ismej.2008.1>
- Rabaey, K., Rozendal, R.A., 2010. Microbial electrosynthesis — revisiting the electrical route for microbial production. *Nat. Rev. Microbiol.* 8, 706–716. <https://doi.org/10.1038/nrmicro2422>
- Ramasamy, R.P., Ren, Z., Mench, M.M., Regan, J.M., 2008. Impact of initial biofilm growth on the anode impedance of microbial fuel cells. *Biotechnol. Bioeng.* 101, 101–108. <https://doi.org/10.1002/bit.21878>
- Richter, H., Nevin, K.P., Jia, H., Lowy, D.A., Lovley, D.R., Tender, L.M., 2009. Cyclic voltammetry of biofilms of wild type and mutant *Geobacter sulfurreducens* on fuel cell anodes indicates possible roles of OmcB, OmcZ, type IV pili, and protons in extracellular electron transfer. *Energy Environ. Sci.* 2, 506–516. <https://doi.org/10.1039/b816647a>
- Roberge, J.K., K., Lundberg, K.H., 2007. *Operational Amplifiers: Theory and Practice*, Second ed. ed. John Wiley & Sons, Ltd. <https://doi.org/10.1109/proc.1976.10358>
- Rowe, A.A., Bonham, A.J., White, R.J., Zimmer, M.P., Yadgar, R.J., Hobza, T.M., Honea, J.W., Ben-Yaacov, I., Plaxco, K.W., 2011. Cheapstat: An open-source, “do-it-yourself” potentiostat for analytical and educational applications. *PLoS One* 6. <https://doi.org/10.1371/journal.pone.0023783>
- Saba, B., Christy, A.D., Yu, Z., Co, A.C., 2017. Sustainable power generation from bacterio-algal microbial fuel cells (MFCs): An overview. *Renew. Sustain. Energy Rev.* 73, 75–84. <https://doi.org/10.1016/j.rser.2017.01.115>
- Schröder, U., Harnisch, F., Angenent, L.T., 2015. Microbial electrochemistry and technology: terminology and classification. *Energy Environ. Sci.* 8, 513–519.
- Schwan, H.P., 1968. Electrode polarization impedance and measurements in biological materials. *Ann. New York Acad. Sci.* 148, 191–209.
- Selembo, P.A., Merrill, M.D., Logan, B.E., 2009. The use of stainless steel and nickel alloys as low-cost cathodes in microbial electrolysis cells. *J. Power Sources* 190, 271–278. <https://doi.org/10.1016/j.jpowsour.2008.12.144>
- Shen, L., Ma, J., Song, P., Lu, Z., Yin, Y., Liu, Y., Cai, L., Zhang, L., 2016. Anodic concentration loss and impedance characteristics in rotating disk electrode microbial fuel cells. *Bioprocess Biosyst. Eng.* 39, 1627–1634. <https://doi.org/10.1007/s00449-016-1638-1>
- Srikanth, S., Venkata Mohan, S., 2012. Change in electrogenic activity of the microbial fuel cell (MFC) with the

function of biocathode microenvironment as terminal electron accepting condition: Influence on overpotentials and bio-electro kinetics. *Bioresour. Technol.* 119, 241–251. <https://doi.org/10.1016/J.BIORTECH.2012.05.097>

- Su, L., Jia, W., Hou, C., Lei, Y., 2011. Microbial biosensors: A review. *Biosens. Bioelectron.* 26, 1788–1799. <https://doi.org/10.1016/j.bios.2010.09.005>
- Sun, J.J., Zhao, H.Z., Yang, Q.Z., Song, J., Xue, A., 2010. A novel layer-by-layer self-assembled carbon nanotube-based anode: Preparation, characterization, and application in microbial fuel cell. *Electrochim. Acta* 55, 3041–3047. <https://doi.org/10.1016/j.electacta.2009.12.103>
- ter Heijne, A., Hamelers, H.V.M., Saakes, M., Buisman, C.J.N., 2008. Performance of non-porous graphite and titanium-based anodes in microbial fuel cells. *Electrochim. Acta* 53, 5697–5703. <https://doi.org/10.1016/j.electacta.2008.03.032>
- Torres, C.I., Krajmalnik-Brown, R., Parameswaran, P., Marcus, A.K., Wanger, G., Gorby, Y.A., Rittmann, B.E., 2009. Selecting anode-respiring bacteria based on anode potential: Phylogenetic, electrochemical, and microscopic characterization. *Environ. Sci. Technol.* 43, 9519–9524. <https://doi.org/10.1021/es902165y>
- Vanmaekelbergh, D., Houtepen, A.J., Kelly, J.J., 2007. Electrochemical gating: A method to tune and monitor the (opto)electronic properties of functional materials. *Electrochim. Acta* 53, 1140–1149. <https://doi.org/10.1016/j.electacta.2007.02.045>
- Varia, J., Martínez, S.S., Orta, S.V., Bull, S., Roy, S., 2013. Bioelectrochemical metal remediation and recovery of Au^{3+} , Co^{2+} and Fe^{3+} metal ions. *Electrochim. Acta* 95, 125–131. <https://doi.org/10.1016/j.electacta.2013.02.051>
- Venkata Mohan, S., Nagendranatha Reddy, C., Naresh Kumar, A., Annie Modestra, J., 2013. Relative performance of biofilm configuration over suspended growth operation on azo dye based wastewater treatment in periodic discontinuous batch mode operation. *Bioresour. Technol.* 147, 424–433. <https://doi.org/10.1016/j.biortech.2013.07.126>
- Wang, K., Sheng, Y., Cao, H., Yan, K., Zhang, Y., 2017. Impact of applied current on sulfate-rich wastewater treatment and microbial biodiversity in the cathode chamber of microbial electrolysis cell (MEC) reactor. *Chem. Eng. J.* 307, 150–158. <https://doi.org/10.1016/j.cej.2016.07.106>
- Wang, X., Feng, Y., Ren, N., Wang, H., Lee, H., Li, N., Zhao, Q., 2009. Accelerated start-up of two-chambered microbial fuel cells: Effect of anodic positive poised potential. *Electrochim. Acta* 54, 1109–1114. <https://doi.org/10.1016/j.electacta.2008.07.085>
- Watson, V.J., Logan, B.E., 2011. Analysis of polarization methods for elimination of power overshoot in microbial fuel cells. *Electrochem. commun.* 13, 54–56. <https://doi.org/10.1016/J.ELECOM.2010.11.011>
- Whitlock, B., 2008. Understanding, finding and eliminating ground loops.
- Yang, Y., Xu, M., Guo, J., Sun, G., 2012. Bacterial extracellular electron transfer in bioelectrochemical systems. *Process Biochem.* 47, 1707–1714. <https://doi.org/10.1016/j.procbio.2012.07.032>
- Yates, M.D., Engel, S.B., Eddie, B.J., Lebedev, N., Malanoski, A.P., Tender, L.M., 2018. Redox-gradient driven electron transport in a mixed community anodic biofilm. *FEMS Microbiol. Ecol.* 1–10. <https://doi.org/10.1093/femsec/fiy081>
- Yin, Q., Zhu, X., Zhan, G., Bo, T., Yang, Y., Tao, Y., He, X., Li, D., Yan, Z., 2016. Enhanced methane production in an anaerobic digestion and microbial electrolysis cell coupled system with co-cultivation of *Geobacter* and *Methanosarcina*. *J. Environ. Sci. (China)* 42, 210–214. <https://doi.org/10.1016/j.jes.2015.07.006>
- You, S., Zhao, Q., Zhang, J., Jiang, J., Wan, C., Du, M., Zhao, S., 2007. A graphite-granule membrane-less tubular air-cathode microbial fuel cell for power generation under continuously operational conditions. *J. Power Sources* 173, 172–177. <https://doi.org/10.1016/j.jpowsour.2007.07.063>
- Zhang, F., Pant, D., Logan, B.E., 2011. Long-term performance of activated carbon air cathodes with different diffusion layer porosities in microbial fuel cells. *Biosens. Bioelectron.* 30, 49–55. <https://doi.org/10.1016/j.bios.2011.08.025>
- Zhang, Y., Merrill, M.D., Logan, B.E., 2010. The use and optimization of stainless steel mesh cathodes in microbial electrolysis cells. *Int. J. Hydrogen Energy* 35, 12020–12028. <https://doi.org/10.1016/j.ijhydene.2010.08.064>
- Zhang, Y., Mo, G., Li, X., Zhang, W., Zhang, J., Ye, J., Huang, X., Yu, C., 2011. A graphene modified anode to improve the performance of microbial fuel cells. *J. Power Sources* 196, 5402–5407. <https://doi.org/10.1016/j.jpowsour.2011.02.067>
- Zhao, F., Slade, R.C.T., Varcoe, J.R., 2009. Techniques for the study and development of microbial fuel cells: an

- electrochemical perspective. *Chem. Soc. Rev.* 38, 1926–1939. <https://doi.org/10.1039/b819866g>
- Zhen, G., Lu, X., Kobayashi, T., Kumar, G., Xu, K., 2016. Promoted electromethanogenesis in a two-chamber microbial electrolysis cells (MECs) containing a hybrid biocathode covered with graphite felt (GF). *Chem. Eng. J.* 284, 1146–1155. <https://doi.org/10.1016/j.cej.2015.09.071>
 - Zhu, N.W., Chen, X., Tu, L.X., Wu, P.X., Dang, Z., 2011. Voltage Reversal during Stacking Microbial Fuel Cells with or without Diodes. *Adv. Mater. Res.* 396–398, 188–193. <https://doi.org/10.4028/www.scientific.net/amr.396-398.188>
 - Zhu, X., Tokash, J.C., Hong, Y., Logan, B.E., 2013. Controlling the occurrence of power overshoot by adapting microbial fuel cells to high anode potentials. *Bioelectrochemistry* 90, 30–35. <https://doi.org/10.1016/j.bioelechem.2012.10.004>
 - Zou, Y., Xiang, C., Yang, L., Sun, L.X., Xu, F., Cao, Z., 2008. A mediatorless microbial fuel cell using polypyrrole coated carbon nanotubes composite as anode material. *Int. J. Hydrogen Energy* 33, 4856–4862. <https://doi.org/10.1016/j.ijhydene.2008.06.061>